

the effect of disorder and of the problem of Anderson localization by using standard techniques.<sup>14-16</sup>

<sup>1</sup>N. Mott, *Philos. Mag.* **6**, 287 (1961).

<sup>2</sup>T. Matsubara and Y. Toyozawa, *Prog. Theor. Phys.* **26**, 739 (1961).

<sup>3</sup>N. Mott, *J. Phys. (Paris)*, Colloq. **37**, C4-301 (1976).

<sup>4</sup>E. Wigner and F. Seitz, *Phys. Rev.* **43**, 804 (1933), and *Phys. Rev.* **46**, 509 (1934).

<sup>5</sup>W. Kohn and L. Sham, *Phys. Rev.* **140**, A1133 (1965).

<sup>6</sup>We use as units of length, energy, and concentration, respectively, the effective Bohr radius  $a_0 = \kappa \hbar^2 / m^* e^2$ , the effective Rydberg  $R = m^* e^4 / 2 \kappa^2 \hbar^2$ , and the concentration  $n_0 = (\pi/3) (4a_0)^{-3}$ , and as reduced temperature  $\theta = kT/R$ .

<sup>7</sup>O. Gunnarsson and B. Lundqvist, *Phys. Rev. B* **13**,

4274 (1976).

<sup>8</sup>See, e.g., H. Woodbury and M. Aven, *Phys. Rev. B* **9**, 5195 (1974).

<sup>9</sup>P. Leroux Hugon and A. Ghazali, *Phys. Rev. B* **14**, 602 (1976).

<sup>10</sup>T. Castner, N. Lee, G. Cieloszyk, and G. Salinger, *Phys. Rev. Lett.* **34**, 1627 (1975).

<sup>11</sup>J. Marko, J. Harrison, and J. Quirt, *Phys. Rev. B* **10**, 2448 (1974).

<sup>12</sup>W. Sasaki, *J. Phys. (Paris)*, Colloq. **37**, C4-307 (1976).

<sup>13</sup>S. Geschwind, R. Romestain, and G. Devlin, *J. Phys. (Paris)*, Colloq. **37**, C4-313 (1976).

<sup>14</sup>F. Yonezawa, M. Watabe, M. Nakamura, and Y. Ishida, *Phys. Rev. B* **10**, 2322 (1974).

<sup>15</sup>P. Antoniou and E. Economou, *Phys. Rev. B* **16**, 3768 (1977).

<sup>16</sup>R. Abou-Chacra, P. Anderson, and D. Thouless, *J. Phys. C* **6**, 1734 (1973).

## First Study of Nuclear Antiferromagnetism by Neutron Diffraction

Y. Roinel, V. Bouffard, G. L. Bacchella, M. Pinot, P. Mériel, P. Roubeau, O. Avenel, M. Goldman, and A. Abragam

*Service de Physique du Solide et de Résonance Magnétique, Centre d'Etudes Nucléaires de Saclay, 91 190 Gif-sur-Yvette, France*

(Received 19 September 1978)

Antiferromagnetic structures of nuclear spins of <sup>7</sup>Li and <sup>1</sup>H have been produced in a single crystal of lithium hydride by the now standard method of dynamic nuclear polarization followed by an adiabatic demagnetization in the rotating frame (ADRF). The (110) Bragg reflection, characteristic of an antiferromagnetic superstructure, has been observed by neutron diffraction. Its line shape and linewidth have been measured, and the sublattice polarizations studied as a function of variables related to the energy and the entropy of the nuclear spins.

This Letter presents the first study of long-range order in a nuclear antiferromagnetic structure, made by neutron diffraction at the EL-3 reactor of Saclay.<sup>1</sup>

Since 1969 when nuclear antiferromagnetism was produced for the first time,<sup>2</sup> numerous studies of the ordered nuclear states have been performed by NMR,<sup>3</sup> on samples of calcium fluoride (CaF<sub>2</sub>), where the <sup>19</sup>F nuclei form a simple-cubic lattice of spins  $\frac{1}{2}$ . A new stage has now been reached with the neutron diffraction experiments in LiH.

The principle and actual methods for producing and studying a dipolar ordered state of the nuclear spins of a diamagnetic crystal have been discussed in a review article,<sup>3</sup> and only its essential aspects are recalled briefly below:

(1) Because of the weakness of the nuclear magnetic moments, the critical temperature  $T_c$  of the ordering is in the microkelvin range.

(2) It is possible to cool the nuclei alone, by dynamic polarization in a high field  $H_0$ , followed by an adiabatic demagnetization in the same dc field by means of radiofrequency fields (ADRF). One can thus observe the ordered state by the techniques of NMR.

(3) The spin temperature  $T$  thus obtained can be either positive or negative, and its absolute value is much lower than that  $T_L$  of the other degrees of freedom of the sample (the "lattice"). The higher is the ratio  $H_0/T_L$ , the smaller the thermal coupling of the spins with the lattice, and the longer the lifetime of the ordered state.

(4) The structure obtained by demagnetization in high field depends on the orientation of  $H_0$  with respect to the crystalline axes, and on the sign of the spin temperature.

(5) Thanks to a spin-dependent term in the neutron-nucleus scattering amplitude, resulting from a nuclear rather than magnetic interaction, the

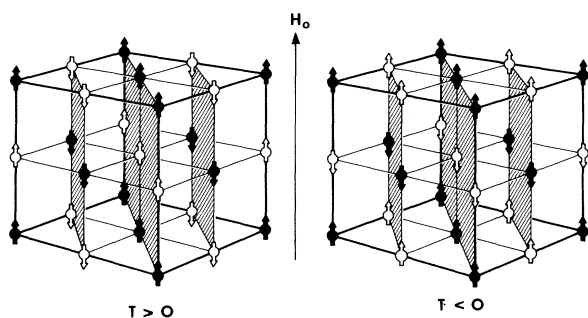


FIG. 1. Nuclear antiferromagnetic structures in LiH for  $\vec{H} \parallel [100]$ . Black and white arrows stand for  ${}^7\text{Li}$  and  ${}^1\text{H}$  nuclei, respectively.

neutron can "tell" the difference between two different sublattices of opposite polarizations, giving rise to superstructure diffraction lines characteristic of long-range antiferromagnetic order. The strength of this interaction can be conveniently described by a fictitious magnetic moment  $\mu^*$ ,<sup>4</sup> expressed in Bohr magneton units  $\mu_B$ . The abnormal weakness<sup>5</sup> of  $\mu^*({}^{19}\text{F}) = -1.8 \times 10^{-2} \mu_B$  was the incentive for studying substances other than  $\text{CaF}_2$ ,<sup>6</sup> and especially LiH,<sup>7</sup> since  $\mu^*({}^1\text{H}) = +5.4 \mu_B$  is the largest of all nuclear  $\mu^*$ .

The crystal structure of LiH is made of two interpenetrating fcc lattices of  ${}^7\text{Li}$  nuclei (spin  $\frac{3}{2}$ ) and  ${}^1\text{H}$  nuclei (spin  $\frac{1}{2}$ ). The ordered superstructures were predicted using a Weiss mean-field approximation. They are shown in Fig. 1 in the case (our experiment) where  $H_0$  is parallel to a  $[100]$  direction. One can see that the  $(110)$  reflection, which is forbidden in the paramagnetic state, becomes allowed in the antiferromagnetic state.

A special apparatus was built for this experiment, including a 6.5-T split-coil magnet with a homogeneity of  $5 \times 10^{-6}$  in a 6-mm  $\times$  6-mm cylinder, a dilution refrigerator of the same type as that of Ref. 7, and a neutron spectrometer. The sample is a single crystal of 5.2 mm  $\times$  4.5 mm  $\times$  0.50 mm, cleaved along  $(100)$  planes. It is doped with a small amount of  $F$  centers ( $2 \times 10^{19} \text{ cm}^{-3}$ ) for the needs of the dynamic polarization. The neutron wavelength is 1.134 Å.

The experimental procedure is the following: A microwave field of frequency 182 GHz saturates off center the ESR line of the  $F$  centers. The maximum nuclear polarization obtained by this method is 80% for  ${}^7\text{Li}$  and 95% for  ${}^1\text{H}$  after 3 days. The microwaves are then switched off, and the temperature of the bath goes down to 50

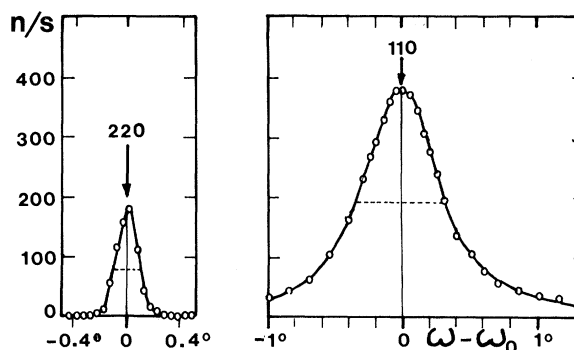


FIG. 2. Neutron counts for the  $(220)$  and  $(110)$  diffraction lines, as a functions of the sample rotation  $\omega - \omega_0$ . The background has been subtracted.

mK. There is no direct measurement of the temperature  $T_L$  of the crystalline lattice. The crystal and counter are placed in the  $(110)$  reflection position, before the antiferromagnetic state is produced by the demagnetization (using radio-frequency fields carefully adjusted to 107.676 MHz for  ${}^7\text{Li}$  and 277.054 MHz for  ${}^1\text{H}$ ). The absolute value of the nuclear spin temperature is at this time about 1  $\mu\text{K}$ . Almost all the experiments reported below correspond to a negative spin temperature (the transition entropy being higher than at positive temperature).

(A) *Line shape.*—Figure 2 shows the shape of the  $(110)$  peak, obtained immediately after the demagnetization. It is Lorentzian with a width at half height of 0.65 deg. The width of the  $(220)$  line, shown for comparison on the same figure at zero nuclear polarization, is only 0.20 deg. We attribute the extra width of the  $(110)$  line to the presence of antiferromagnetic domains of size

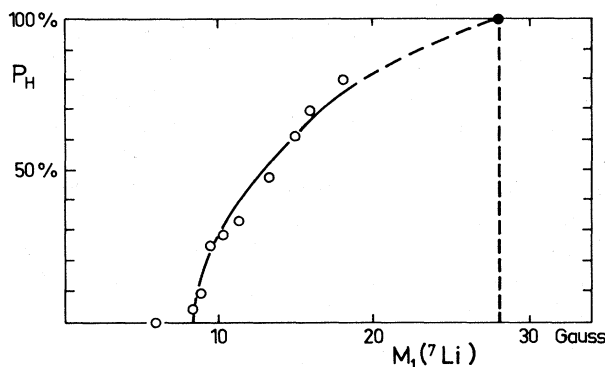


FIG. 3. Proton sublattice polarization  $p_H$  as a function of the NMR first moment of  ${}^7\text{Li}$ . The black point corresponds to the limit  $T = 0$  in the Weiss approximation.

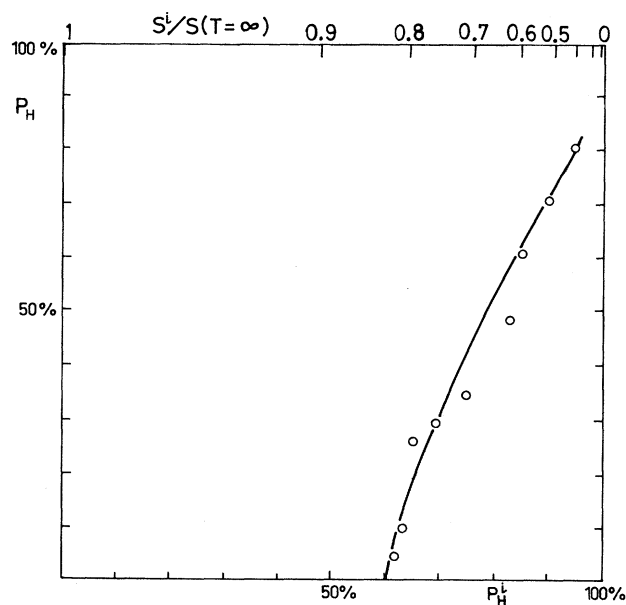


FIG. 4. Proton sublattice polarization  $P_H$  as a function of the proton initial polarization  $P_H^i$ , and of the total initial entropy ( $^1\text{H}$  and  $^7\text{Li}$ ).

100–200 Å. The (110) line decays with a characteristic time of 1 h, comparable to the NMR dipolar relaxation time. As expected, it disappears with the long-range antiferromagnetic order, well before complete warm-up of the nuclear spins. No noticeable change can be detected in the line shape and linewidth in the course of the relaxation.

(B) *Intensity*.—For  $T < 0$ , the intensity of the (110) line should vary as

$$F_{\text{af}}^2 = \left(\frac{1}{2}B_H P_H - \frac{3}{2}B_{\text{Li}} P_{\text{Li}}\right)^2, \quad (1)$$

where  $P_H$  and  $P_{\text{Li}}$  are the sublattice polarizations, and  $B_H = +2.91 \times 10^{-12}$  cm and  $B_{\text{Li}} = -0.11 \times 10^{-12}$  cm are the spin-dependent neutron-scattering amplitudes. The actual intensity varies, in fact, more slowly than (1), because of extinction. The calibration of the (110) reflection was made by assuming the same extinction law as that measured in a separate experiment on the (220) reflection. The proton sublattice polarizations are then deduced from the intensities, taking a ratio of  $P_{\text{Li}}/P_H$  equal to its theoretical value in the Weiss approximation (roughly 0.7). It turns out that the dipolar relaxation is not homogeneous in the sample. A relative homogeneity of the spin temperature in the sample is achieved either by starting the demagnetization from various nuclear polarizations, or by performing partial rf saturations of the spins in a time short compared with the

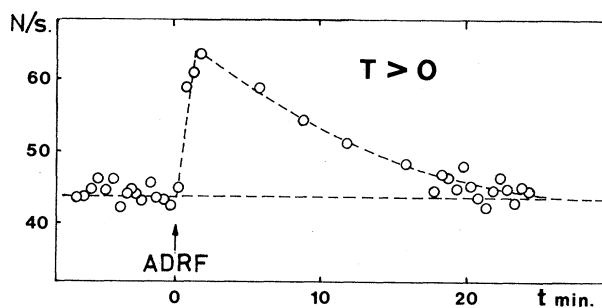


FIG. 5. Neutron counts for the (110) reflection as a function of time  $t$  for positive temperature.

shortest relaxation time. The proton sublattice polarization  $P_H$  is plotted in Fig. 3 as a function of the first moment of the  $^7\text{Li}$  NMR signal (an increasing function of energy and inverse temperature<sup>2</sup>). In Fig. 4,  $P_H$  is plotted as a function of the initial proton polarization  $P_H^i$ , and of the initial total entropy. The critical value of  $P_H^i$  is about 60% in this sample.

(C) *Positive temperature*.—In a preliminary experiment, a (110) reflection has also been observed at positive temperature, with  $P_H^i = 95\%$  and  $P_{\text{Li}}^i = 80\%$ . The neutron signal was about 25 times smaller than at negative temperature for the same conditions. Figure 5 shows the neutron signal at the center of the line, as a function of time  $t$  after the demagnetization.

With neutron diffraction, which gives direct access to long-range nuclear ordering, the studies of nuclear antiferromagnetism take up a new dimension.

<sup>1</sup>A brief report of a preliminary experiment has been given earlier [A. Abragam, G. L. Bacchella, V. Bouffard, M. Goldman, P. Mériel, M. Pinot, Y. Roinel, and P. Roubeau, C. R. Acad. Sci. (Paris) **286**, B311 (1978)].

<sup>2</sup>M. Chapellier, M. Goldman, Vu Hoang Chau, and A. Abragam, C. R. Acad. Sci. (Paris) **268**, 1530 (1969).

<sup>3</sup>M. Goldman, Phys. Rep. **32C**, 1 (1977).

<sup>4</sup>A. Abragam, G. L. Bacchella, H. Glättli, P. Mériel, J. Piesvaux, and M. Pinot, C. R. Acad. Sci. (Paris) **274**, 423 (1972).

<sup>5</sup>A. Abragam, G. L. Bacchella, C. Long, P. Mériel, J. Piesvaux, and M. Pinot, J. Phys. (Paris), Lett. **36**, L236 (1972).

<sup>6</sup>S. F. J. Cox, V. Bouffard, and M. Goldman, J. Phys. C **8**, 3664 (1975).

<sup>7</sup>Y. Roinel, V. Bouffard, and P. Roubeau, to be published.